Cellular/Molecular

Progressive Deafness and Altered Cochlear Innervation in Knock-Out Mice Lacking Prosaposin

Omar Akil,[1] Jolie Chang,[1] Hakim Hiel,[2] Jee-Hyun Kong,[3] Eunyoung Yi,[2] Elisabeth Glowatzki,[2] and Lawrence R. Lustig[1]

[1]Department of Otolaryngology–Head and Neck Surgery, University of California, San Francisco, San Francisco, California 94143-0449, [2]Department of Otolaryngology–Head and Neck Surgery, Johns Hopkins School of Medicine, Baltimore, Maryland 21287, and [3]Department of Neuroscience, Johns Hopkins School of Medicine, Baltimore, Maryland 21205

After a yeast two-hybrid screen identified prosaposin as a potential interacting protein with the nicotinic acetylcholine receptor (nAChR) subunit α10, studies were performed to characterize prosaposin in the normal rodent inner ear. Prosaposin demonstrates diffuse organ of Corti expression at birth, with gradual localization to the inner hair cells (IHCs) and its supporting cells, inner pillar cells, and synaptic region of the outer hair cells (OHCs) and Deiters' cells (DCs) by postnatal day 21 (P21). Microdissected OHC and DC quantitative reverse transcriptase-PCR and immunohistology localizes prosaposin mRNA to DCs and OHCs, and protein predominantly to the apex of the DCs. Subsequent studies in a prosaposin knock-out (KO) (−/−) mouse showed intact but slightly reduced hearing through P19, but deafness by P25 and reduced distortion product otoacoustic emissions from P15 onward. Beginning at P12, the prosaposin KO mice showed histologic organ of Corti changes including cellular hypertrophy in the region of the IHC and greater epithelial ridge, a loss of OHCs from cochlear apex, and vacuolization of OHCs. Immunofluorescence revealed exuberant overgrowth of auditory afferent neurites in the region of the IHCs and proliferation of auditory efferent neurites in the region of the tunnel of Corti. IHC recordings from these KO mice showed normal *I–V* curves and responses to applied acetylcholine. Together, these results suggest that prosaposin helps maintain normal innervation patterns to the organ of Corti. Furthermore, prosaposin's overlapping developmental expression pattern and binding capacity toward the nAChR α10 suggest that α10 may also play a role in this function.

Key words: **acetylcholine receptor; AchR; afferent; auditory; auditory nerve; cochlea; development; efferent; hair cells; neurotropic; nicotinic receptor; prosaposin; saposin**

Introduction

Mechanosensory hair cells of the organ of Corti transmit information regarding sound to the CNS by way of peripheral afferent neurons. The CNS feeds back and regulates this process through efferent cholinergic neurons (the olivocochlear pathway). This efferent system can be subdivided into the lateral efferents that terminate on the afferent dendrites innervating the inner hair cells (IHCs), and the medial efferents that directly terminate onto IHCs (only during development), and later directly onto outer hair cells (OHCs) (Simmons, 2002). Activation of the efferent system, either by sound or by direct electrical stimulation, is inhibitory, causing reduced tuning and sensitivity of the cochlear afferents (Galambos, 1956; Wiederhold and Kiang, 1970; Klinke and Galley, 1974; Eybalin, 1993).

It is now widely held that efferent-mediated OHC inhibition occurs via activation of the heteromeric nicotinic acetylcholine receptor (nAChR) $\alpha 9\alpha 10$, with subsequent activation of the calcium-activated potassium channel SK2 (Elgoyhen et al., 1994, 2001; Flock and Russell, 1976; Fuchs and Murrow, 1992a,b; Lustig et al., 2001; Martin and Fuchs, 1992). Although this "two-channel" hypothesis remains attractive for describing many aspects of OHC inhibition, it fails to account for other observations, including evidence for a muscarinic pathways of hair cell inhibition (Shigemoto and Ohmori, 1991; Niedzielski and Schacht, 1992; Ogawa et al., 1994). Furthermore, the application of ryanodine has been shown to alter calcium-induced potassium currents in mammals, whereas the ryanodine receptor agonist caffeine has been shown to cause shortening and decreased potassium conductance of OHCs (Slepecky et al., 1988; Skellett et al., 1995; Yamamoto et al., 1995; Evans et al., 2000; Baker et al., 2004; Lioudyno et al., 2004).

Together, these studies suggest that activation of the nAChR $\alpha 9\alpha 10$ may have more complicated downstream effects than hypothesized previously. Studies in OHCs by Sridhar et al. (1997) demonstrating variable mechanisms of calcium activation of the SK channel after nAChR activation support this notion. If true, it might be expected that the activation of nAChR $\alpha 9\alpha 10$ by acetylcholine could mediate some of these downstream effects directly through protein-protein interactions.

To test this hypothesis, the intracellular (IC) loop of the nAChR subunit α10 was used as bait in a yeast two-hybrid screen of a rat cochlear cDNA library. One of the interacting binding

Received Feb. 17, 2005; revised Nov. 10, 2006; accepted Nov. 13, 2006.

This work was supported by National Institute on Deafness and Other Communication Disorders Grants K08 DC00189 (L.R.L.), R01 DC006476, and P30 DC05211 and by generous financial support from Vernon Wright. We also acknowledge manuscript comments and suggestions from Dr. Paul A. Fuchs, as well as the prosaposin knock-out mice and prosaposin antibody from the laboratory of Dr. Greg Grabowski at the University of Cincinnati (Cincinnati, OH).

Correspondence should be addressed to Lawrence R. Lustig, Department of Otolaryngology–Head and Neck Surgery, University of California, San Francisco, U401, Box 0449, 533 Parnassus Avenue, San Francisco, CA 94143-0449. E-mail: llustig@ohns.ucsf.edu.

DOI:10.1523/JNEUROSCI.3746-06.2006

 0270-6474/06/2613076-13$15.00/0

partners identified was prosaposin, a precursor glycoprotein of four sphingolipid activator proteins, saposins A–D (O'Brien et al., 1988). To date, neither prosaposin nor saposin functional activity has been reported in the ear or to be involved in the maintenance of hearing.

This current study characterizes prosaposin within the rat cochlea and reports on the anatomical and functional results in the organ of Corti when prosaposin function is abolished in a knock-out (KO) mouse (Sun et al., 2002). Together, the findings in this study have implications for our understanding of the development and maintenance of hearing.

Materials and Methods

Yeast two-hybrid screening

A genetic screen using an enhanced Gal4 two-hybrid system (Matchmaker System 3; BD Clontech, Palo Alto, CA) was performed as recommended by the manufacturer's protocol, using the intracellular loops of the rat nAChR α9 and α10 as "bait" against a rat cochlear cDNA library. The rat nicotinic acetylcholine receptors α9 (380 bp) and α10 (279 bp) intracellular loops were PCR amplified and subcloned into the Gal4 DNA binding domain yeast expression vector pGBK T7. The resulting expression vector was transformed into the haploid Y187 competent yeast strain using the lithium acetate method and used as a bait to screen an oligo(dT) cDNA library generated from 0.17 μg of polyA RNA purified from 20 cochleas of 3- to 4-week-old rats using Trizol (Invitrogen, Carlsbad, CA) for total RNA extraction and oligotex mRNA Mini kit (Qiagen, Valencia, CA) to purify mRNA. The cDNAs were PCR amplified and then purified using a Chroma Spin-400 column (Clontech) to pool cDNAs of 0.5 kb or longer, and then subcloned into the Gal4 DNA activating domain pGADT7-Rec expression vector before transformation into the haploid yeast strain AH109.

Yeast screening for potential interacting proteins with nAchRs α9 and α10 was performed by mating Y187 α9 or α10 pGBKT7 and AH109 rat cochlea cDNA library pGADT7-Rec. Transformed colonies were selected on SD-Ade/-His/-Leu/-Trp+X-α-gal media by selecting blue colonies indicative of a potentially positive interaction between the bait (α9 and α10) and the prey (library protein). Potential positive clones were restreaked several times on SD-Leu/-Trp+X-α-gal plates, then replica plated on maximally selective SD-Ade/-His/-Leu/-Trp+X-α-gal media to ensure that colonies contained the correct phenotype. The colonies that successfully passed the reporter test were harvested for plasmid isolation using a yeast plasmid isolation kit (USB, Cleveland, OH). AD clones were recovered by selecting on Luria broth agar plates supplemented with ampicillin. Resulting colonies were grown overnight and plasmid DNA were analyzed by restriction mapping using *Hae*III (New England Biolabs, Ipswich, MA) and sequenced to identify the insert in pGADT7-Rec vector representing the putative interaction protein. Candidate interacting protein sequences were then Blasted (http://www.ncbi.nlm.nih.gov/BLAST/) for sequence identity.

In vitro coimmunoprecipitation (co-IP) was used to independently confirm putative protein–protein interactions. After detecting protein–protein interactions through the *in vivo* yeast two-hybrid screen, the vectors were used directly in the *in vitro* transcription–translation reaction that was performed by using the rabbit reticulocyte lysate system (TNT kit; Promega, Madison, WI) according to the manufacturer's instructions. The reaction was incubated for 90 min at 30°C in the presence of S^{35} methionine. The product proteins (S^{35}-α10 + cMyc tag and S^{35}-prosaposin + AH tag) were mixed, split into two tubes, and incubated for 1 h at room temperature. The anti-AH antibody was then added to one of the tubes and the anti-cMyc antibody to the other tube. The complex was isolated after a 1 h incubation at room temperature by binding to protein A beads. The beads were washed following the manufacturer's instructions and resuspended in Lammli buffer, heated for 5 min at 80°C, and electrophoresed in 15% SDS-PAGE gel. Kodak (Rochester, NY) x-ray films were exposed on the dry gels and developed, or the dry gel was visualized by autoradiography.

To more precisely localize the prosaposin and α10 binding region, primers with appropriate restriction digest sites were designed to span varying lengths of the prosaposin protein. These PCR products were then subcloned into the pGAD vector. Yeast two-hybrid screens as described above were then performed with the intracellular loop of nAChR α10 to determine binding interaction.

Outer hair cell RT-PCR

Isolated OHC reverse transcriptase (RT)-PCR was used to confirm the presence of prosaposin from microdissected populations of isolated cochlear OHCs. For single cell isolation, sections of the apical turns of the organ of Corti from 13- to 14-d-old Sprague Dawley rats were dissected and placed in a sterile saline solution [containing the following (in mM): pH 7.4, 6.8 KCl, 144 NaCl, 0.9 MgCl2, 1.3 CaCl2, 0.7 NaH_2PO_4, 5.6 D-glucose, 10 HEPES] and viewed under an Axioscope (Zeiss, Oberkochen, Germany) with a 63× water-immersion objective using a camera with contrast enhancement. Manipulations were done under a fast flow of sterile saline solution. The pipettes for isolation of the cell content had a large tip diameter so that the whole cell content could be aspirated (rather than patch clamped). The pipettes tip were backfilled with the extraction buffer (Arcturus, Mountain View, CA) that both lyses the cells and preserves RNA from degradation. Outer hair cells were sequentially aspirated into the isolation pipette. Next, the pipette tip was broken into a 0.5 ml tube, spun down briefly in a microcentrifuge, and the supernatant of hair cells lysates were applied to Picopure columns (Arcturus). Contaminating DNA was digested in the Picopure column using RNase-free DNase I (Qiagen) for 20 min at 37°C. The total RNA was purified following the manufacturer's instructions (Arcturus).

The total RNA harvested from the OHC extractions was reverse transcribed with superscript II RNase H (Invitrogen) for 50 min at 42°C, using reverse primers of prosaposin (GGAGCCCCCTTTTGTCTTCCCCC) combined with the reverse primer of nAChR α9 (ccagcgtgtgagttcagctgc) (used as a positive control for the presence of OHCs in the sample). Two microliters of RT reaction product were used for subsequent PCR (*Taq*DNA polymerase; Promega) of 35 cycles using the following parameters: 94°C for 30 s, 60°C for 45 s, 72°C for 1 min, followed by a final extension of 72°C for 10 min, and storage at 4°C. Primers were designed to amplify a unique sequence of rat prosaposin (604 bp) and a unique sequence of the rat nAChR α9 subunit (315 bp) after a second round PCR. First-round PCR primers used were as follows: prosaposin forward, gcgcgccatgtatgctctcgctc; prosaposin reverse, ccagcttgcagaagtcgcctac; α9 forward, gccacgccaggagccagaaca; and α9 reverse, ccagcgtgtgagttcagctgc. Second-round PCR primers were as follows: prosaposin forward, aggaggattgtgaccgcctcggg; prosaposin reverse, gaagagccaagcagtctgcattgcgc; α9 forward, acttggggtaccagggtgggat; and α9 reverse, ctgagatctgccccagcgtgtga. Controls included single-cell RNA preparation without reverse transcriptase as well as samples of the background saline solution bathing the OHCs during isolation.

Analysis of each PCR sample was then performed on 2% agarose gels containing 0.5 μg/ml ethidium bromide. Gels were visualized using a digital camera and image processing system (Kodak). Candidate bands were cut out and the DNA was extracted (Qiaquick gel extraction kit; Qiagen) and sequenced (Johns Hopkins DNA analysis facility, Baltimore, MD). The PCR product was then compared directly to the full rat prosaposin for sequence identity.

Microdissected OHC and Deiters' cell quantitative RT-PCR

For real-time quantitative RT-PCR, OHCs and Deiters' cells (DCs) were individually microdissected and pooled as separate populations, as described above. RNA was extracted and processed, also as described above. The expression level of prosaposin, α9 and α10 was measured by the iQ5 real time PCR (Bio-Rad, Hercules, CA). Amplification was performed in a total volume of 25 μl containing 12.5 μl SYBR Green I amplification master mix (Bio-Rad), 250 nM of each forward primer (prosaposin, 5′gcctcctcagaagaacgggggg 3′; α9, 5′ acctggggtaccagggtgggat 3′; α10, 5′ ggctggacctgttgtcctacatcg 3′; and ribosomal protein L19, 5′atgtatcacagcctgtacctg 3′) and reverse primer (prosaposin, 5′ gtaggcgacttctgcaagctgg 3′; α9, 5′ ccagcgtgtgagttcagctgc 3′; α10, 5′tggctgcgtgtccgccttgtt 3′; and ribosomal protein L19, 5′ttcttggtctcttcctccttg 3′), and 1 μl of OHC or DC cDNA as template. The amplifications were always performed in triplicate wells, using a program that consisted of initial denaturation at 95°C

for 3 min followed by a 40 cycles of denaturation at 95°C for 10 s and annealing at 61°C for 30 s. After amplification, a melting curve was generated for every PCR product to check the specificity of the PCR (absence of primer dimers or other nonspecific amplification product). The threshold cycle (Ct) values were determined and the compared Ct value of the ribosomal protein L19 used as a house keeping gene measured in the same sample. Values for each were expressed as fold amplification over L19. Statistical differences were calculated using a two-tailed paired Student's *t* test, with significance noted for $p < 0.05$.

Rat prosaposin immunohistology

Sprague Dawley rats at varying time points [postnatal day 1 (P1), P5, P10, P15, P21, P30] were anesthetized, and their cochleae were isolated, dissected, perfused through the round window by 2% paraformaldehyde in 0.1 M phosphate buffer (PB) at pH 7.4, and incubated in the same fixative for 2 h. After fixation, cochleas were rinsed with PB and immersed in 5% EDTA in 0.1 M PB for decalcification. When cochleas where totally decalcified (~3 d), they were incubated overnight in 30% sucrose for cryoprotection. The cochleas then were embedded in OCT Tissue Tek compound (Miles Scientific, Naperville, IL). Tissues were cryosectioned at 10–12 μm thickness for immunohistochemistry, mounted on Superfrost microscope slides (Erie Scientific, Portsmouth, NH) and stored at −20°C until use.

For immunofluorescent staining of the normal rat cochlea, a rabbit polyclonal prosaposin antibody was made toward the C-terminal end of mouse prosaposin, corresponding to saposin D (generously provided by Dr. Greg Grabowski, University of Cincinnati, Cincinnati, OH). The antibody was created by subcloning the coding region of saposin D into a pET vector, overexpressing in *Escherichia coli*, and then purification of the antibody on a nickel column, as described previously (Leonova et al., 1996). Polyclonal antibodies toward saposin D were then raised in New Zealand white rabbits. In some experiments, 4,6-diamidino-2-phenylindole (DAPI) was also used as a double label to identify cell nuclei. After incubation at 37°C for 30 min, the sections were rinsed twice for 5 min in 0.1 M PBS, pH7.4, and then preincubated for 1 h in 0.3% Triton X-100 and 30% normal goat serum (NGS). The sections where then incubated in a humid chamber overnight at 4°C with anti-prosaposin antibody (1:200) diluted in PBS. Slides were then rinsed (two times for 10 min) and incubated for 2 h in goat anti-rabbit IgG conjugated to Cy2 or Cy3 diluted to 1:3000. The sections were rinsed in PBS (two times for 10 min) and mounted in equal parts glycerol/PBS and coverslipped. Slides treated with the same technique but without incubation in the primary antibody were used as a control. Slides were observed with a Zeiss microscope with epifluorescence equipment.

For double and triple labeling along with prosaposin, tissue sections were prepared as described above and slides were observed with an Olympus (Tokyo, Japan) microscope with confocal immunofluorescence. Additional markers and antibodies for staining were used as follows. For phalloidin, after the removal of the secondary antibodies and before the final washes, sections were stained with rhodamine phalloidin (Invitrogen) from a stock solution of 200 U/ml methanol and diluted 1:100 in PBS for 50 min. For synaptophysin, mouse anti-synaptophysin monoclonal antibody (Millipore, Billerica, MA) was used at 1:500 dilution and incubated over night at 4°C. For choline acetyl transferase (ChAT; Millipore), goat anti-choline acetyltransferase affinity purified polyclonal antibody was used at 1:75 and incubated over night at 4°C. In some cases the fluorescent dye DAPI (1.5 μg/ml in PBS; Sigma, St. Louis, MO) was also used to counterstain nuclei. After the removal of the secondary antibodies and before the final washes, the sections were exposed for 15 min at room temperature to DAPI; staining allowed visualization of the nuclei together with immunofluorescence.

Knock-out mouse histopathology

Light microscopy. Prosaposin knock-out mice (generously provided by Dr. Greg Grabowski) (Sun et al., 2002) ranging from P12 to P30 were anesthetized and their cochleae were isolated, dissected, perfused through the round window with both 2% paraformaldehyde and 2% glutaraldehyde in 0.1 M phosphate buffer, pH 7.4, and then incubated in the same fixative overnight at 4°C. The cochleae were rinsed with 0.1 M PB and post fixed in 1% osmium tetroxide for 1 h. The bone surrounding the cochlea was thinned and the cochlea subsequently immersed in 5% EDTA (0.2 M). The decalcified cochlea were dehydrated in ethanol and propylene oxide and embedded in Araldite 502 resin (Electron Microscopy Sciences, Fort Washington, PA) and sectioned at 15–20 μm. After sections were stained with Toluidine Blue, they were mounted in Permount (Fisher Scientific, Houston, TX) on microscope slides.

Electron microscopy. The cochleae of 21-d-old mice were surgically exposed, a stapedectomy was performed, and the round window perforated. Temporal bones were preserved by gentle *in vivo* perfusion of fixative (1.5% glutaraldehyde and 2.5% paraformaldehyde, buffered to pH 7.4, with 0.1 M phosphate) through the perilymphatic channels, followed by postfixation in 1% phosphate buffered osmium tetroxide with 1.5% potassium ferricyanide. Ferricyanide-reduced osmium was used to improve contrast. Specimens were dissected, dehydrated, and embedded in Epon. Extra-thick block surface preparations containing the spiral ganglion as well as the organ of Corti were mounted on glass slides. The basilar membrane was measured along the tops of the pillar cells and segments of the organ of Corti with the adjacent spiral ganglion were cut from the surface preparation at selected sites with razor blade cuts made parallel to the radial nerve fibers, which are clearly visible through the osseous spiral lamina. These small pieces, containing about a 0.5 mm sector of the basilar membrane and associated spiral ganglion, were remounted and sectioned at l-2 pm in the radial plane. Ultrathin silver to gray sections were collected on Formvar films on slotted grids, stained with saturated aqueous uranyl acetate and lead citrate (0.4% in 0.15N sodium hydroxide), and examined at 60 kV in a JEOL-JEM 100S transmission electron microscope.

Hair cell counts. The cochlea from wild-type (WT) ($n = 5$) and KO ($n = 5$) mice were perfused with 4% PFA in 0.1 M PBS, pH 7.4, and kept in the fixative overnight at 4°C. The cochlea was washed with PBS three times for 10 min and then decalcified with 5% EDTA in 0.1 M PBS for 3 d. After decalcification, the otic capsule was then removed, followed by removal of the lateral wall, tectorial membrane, and Reissner's membrane. The remaining organ of Corti was stained with rhodamine–phalloidin (stock solution of 200 U/ml methanol diluted 1:100 in PBS) for 1 h. Thereafter, the whole mount was rinsed in PBS and further dissected into surface preparation (microdissected into individual turns), and mounted on glass slides in a mounting solution. Hair cells in the organ of Corti were visualized under the microscope equipped with epifluorescence, using a 40× objective. Statistical differences between WT and KO mice were calculated for varying lengths along the cochlea (0.1 mm) using an unpaired Student's *t* test. Statistical significance was defined as $p < 0.05$.

Immunofluorescence. Tissue sections for immunofluorescence were prepared as described above for the rat. For immunofluorescent staining, two antibodies were used: neurofilament-200 (NF-200; Millipore), which labels afferent auditory fibers (Berglund and Ryugo, 1991), and synaptophysin (Zymed, South San Francisco, CA), which labels efferent auditory fibers (Schimmang et al., 2003). After incubation at 37°C for 30 min, the sections were rinsed twice for 5 min in 0.1 M PBS, pH 7.4, and then preincubated for 1 h in either 0.3% Triton X-100 and 30% NGS (NF-200), or 10% NGS without Triton X-100 (synaptophysin). The sections where then incubated in a humid chamber overnight at 4°C with the primary antibody (1:500 NF-200 or 1:200 synaptophysin diluted in PBS). They were then rinsed (two times for 10 min) and incubated for 2 h in goat anti-rabbit IgG conjugated to Cy3 diluted to 1:2000 in PBS. The sections were rinsed in PBS (two times for 10 min) and mounted in equal parts glycerol/PBS and coverslipped. Slides treated with the same technique but without incubation in the primary antibody were used as a control. Slides were observed with a Olympus microscope with confocal immunofluorescence.

Auditory physiology testing

All auditory tests were done in a soundproof chamber. Before acoustic testing, mice were anesthetized with an intraperitoneal injection of a mixture of ketamine hydrochloride (Ketaset, 100 mg/kg) and xylazine

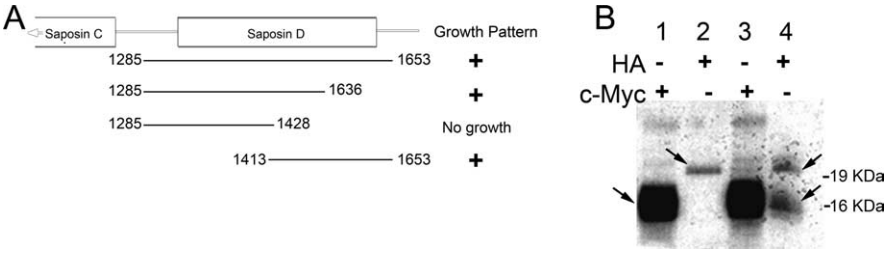

Figure 1. Verification of the yeast two-hybrid interaction. ***A***, Varying lengths of the terminal end of prosaposin (corresponding to saposin D) were used in yeast two-hybrid constructs to test the protein–protein interaction. The region that appears to be primarily responsible for the interaction with nAChR α10 resides between 1428 and 1536 of saposin D. ***B***, *In vitro* co-IP of nAChR α10 and prosaposin. Lane 1 is α10 alone labeled by c-Myc (arrow next to strongly labeled band), probing with a c-Myc antibody. Lane 2 is prosaposin alone labeled by hemagglutinin (HA; arrow), probing with an HA antibody. Lane 3 is a co-IP labeling α10 (strongly) and prosaposin (weakly) probing with the c-Myc antibody. As expected, both bands corresponding to prosaposin and α10 are present. The larger additional bands noted are also seen in lane 1 and represent nonspecific binding of c-myc/α10. Lane 8 is a co-IP labeling both α10 and prosaposin (arrows) probing with the HA antibody. This experiment independently verifies protein–protein binding between the intracellular loop of nAChR α10 and prosaposin.

hydrochloride (Xyla-Ject, 10 mg/kg) with intraperitoneal boosters at one-fifth the original dose as required. Body temperature was maintained with a heating pad and monitored with a rectal probe throughout the recording periods.

ABR testing. Evoked acoustic brainstem response thresholds were differentially recorded from the scalp of knock-out mice at varying ages (~2–4 weeks). Responses were recorded using subdermal needle electrodes at the vertex, below the pinna of the left ear (reference), and below the contralateral ear (ground). The sound stimuli used included click (5 ms duration; 31 Hz) and tone pips at 8, 16, and 32 kHz (10 ms duration; cos2 shaping; 21 Hz). Measurements were done using the TDT BioSig III system. For each stimulus, electroencephalographic activity was recorded for 20 ms at a sampling rate of 25 kHz, filtered (0.3–3 kHz), and waveforms from 512 stimuli were averaged. Auditory brainstem response (ABR) waveforms were recorded in 5 dB sound pressure level (SPL) intervals down from the maximum amplitude. Threshold was defined as the lowest stimulus level at which response peaks for waves I–V were clearly and repeatably present on visual inspection. These threshold judgments were confirmed by analysis of stored waveforms. Data were obtained from 12-, 15-, 19-, 22-, 25-, and 30-d-old wild-type ($n = 4$), heterozygous ($n = 4$), and homozygous null ($n = 4$) mice.

Comparison of each group of animals (wild-type, heterozygote, and mutant homozygote) was performed using one-way ANOVA with Bonferroni *post hoc* testing. Significance was defined at $p < 0.05$. To enable the average and statistical calculations, an unobtainable ABR threshold (no response at 190 db or less) was defined as 90 db.

DPOAE testing. The distortion product otoacoustic emissions (DPOAEs) were measured using an acoustic probe placed in the left external auditory canal. Stimuli consisted of two primary tones (f1/f2 = 1.25) digitally synthesized at 100 kHz using SigGen software. The primary tones with geometric mean (GM) frequencies ranging from 6 to 36 kHz, and equal levels (L1 = L2 = 60 dB SPL) were presented via two separate speakers (EC1; Tucker Davis Technologies, Alachua, FL) to the acoustic probe. DPOAE 2f1–f2 responses were recorded using an ER10B+ (Etymotics Research, Elk Grove Village, IL) microphone assembly within the acoustic probe and the TDT BioSig III system. Responses were amplified, digitally sampled at 100 kHz, and averaged over 50 discrete spectra. Fast Fourier transforms were computed from averaged responses. For each stimulus set, DPOAE amplitude level at 2f1–f2 was extracted and sound pressure levels for data points 100 Hz above and below the DPOAE frequency were averaged for the noise floor measurements. DPOAE level was plotted as a function of primary tone GM frequency. Statistical analysis was done using ANOVA with Bonferroni *post hoc* tests with significance defined as $p < 0.05$. Data were collected from mice at varying ages, including P15, P19, P25, and P30 for wild-type ($n = 4$ each group), heterozygous ($n = 3$ each group), and homozygous null ($n = 3$ each group) mice.

Inner hair cell electrophysiology. Apical turns of the rat organ of Corti were acutely isolated at P7–P11 and P19 and viewed under an Axioscope (Zeiss) with a 63× water-immersion objective using a camera with contrast enhancement. Some cells were removed to access the IHCs, but mostly the pipette moved through tissue under positive pressure. Currents from IHCs were recorded using the whole-cell patch-clamp technique and an Axoclamp 200B amplifier. Five to 10 MΩ electrodes were used and the recordings were done at room temperature [solutions contained the following (in mM): pipette solution, 150 KCl, 3.5 $MgCl_2$, 0.1 $CaCl_2$, 5 EGTA, 5 HEPES, 2.5 Na_2ATP; standard extracellular solution, 5.8 KCl, 155 NaCl, 0.9 $MgCl_2$, 1.3 $CaCl_2$, 0.7 NaH_2PO_4, 5.6 glucose, 10 HEPES]. Solutions containing ACh or extracellular solution with 40 mM potassium (to activate efferent synaptic transmission) were applied via a gravity-fed multichannel glass pipette (~150 μm in diameter) positioned ~300 μm away from the organ of Corti.

Results

Yeast two-hybrid screen results

In an effort to identify potential interacting proteins with the heteromeric nAChR subunits α9 and α10 within OHCs, the IC loops of both receptor subunits were used as bait in a yeast two-hybrid screen. The IC loops were chosen for several reasons: (1) it is primarily the sequence differences in the IC loops of nAChR subunits that distinguish them from one another (Galzi et al., 1991), and (2) the yeast two-hybrid technique necessitates the use of a hydrophilic sequence as part of the screen (McNabb and Guarente, 1996). Although repeated twice, the screen of the α9 IC loop subunit yielded no interacting proteins, implying either the intracellular loop of α9 does not bind to any proteins within the inner ear, or that the library was incomplete. In contrast, the screen with the α10 IC loop resulted in ~200 clones, which were subsequently narrowed to nine unique clones after restriction digest testing. An overwhelming majority of the original duplicate clones coded for a protein not described previously within the inner ear, prosaposin.

Additional studies further localized prosaposin binding in an ~120 bp region, corresponding to a portion of saposin D (Fig. 1*A*). A sequence search of this area demonstrated no known binding motifs (DNAsis software; MiraBio). *In vitro* coimmunoprecipitation was used as an independent verification of nAChR α10 and prosaposin interaction (Fig. 1*B*). As a negative control, the intracellular loop of nAChR α9 was used, and did not demonstrate co-IP interaction (data not shown). This study lends additional support to the veracity of interaction between prosaposin and α10.

Characterization of prosaposin in the inner ear

Immunohistology was used to characterize the expression of prosaposin within the cochlea using rabbit polyclonal antisera directed against the C-terminal end of prosaposin, corresponding to saposin D (Fig. 2) (immunofluorescence labeling thus does not differentiate between prosaposin, an active protein in itself, and its cleaved product saposin D). Immunofluorescence staining from P1 through P30 demonstrates initially diffuse expression of prosaposin that gradually localizes to several discrete locations within the organ of Corti: IHCs and its supporting cells, inner pillar cells, and the synaptic region of the OHCs (either base of OHCs or apex of the DCs).

Based on initial immunofluorescence labeling, we were unable to determine whether prosaposin was expressed in the basal region of the OHCs (which would be consistent with an interaction with the nAChR α10 subunit) and/or expressed in the adjacent apex of the DCs and efferent synaptic cleft. As a result, additional studies were undertaken to further refine the location of prosaposin in this region (Fig. 3). RT-PCR on populations of 50–200 microdissected OHCs clearly demonstrated the presence of both nAChR α9 (positive control) and prosaposin from the same starting RNA sample (Fig. 3*A*). To verify that extracted OHC tissue did not contain contaminants from other cell types, we tested for a gene expressed specifically in DCs, the supporting cells located just beneath the OHCs. DCs, but not OHCs, express the glutamate/aspartate transporter GLAST1 (Furness et al., 2002) and we tested our OHC extract for GLAST1 to verify that the microdissection technique can yield pure populations of OHCs without supporting cell contaminants. As shown (Fig. 3*A*), GLAST1 was not amplified after two rounds of RT-PCR from 200 microdissected OHCs, but was clearly identified in 50 DCs from a similar number of rounds of amplification.

After these studies, additional attempts to localize prosaposin to OHCs and/or DCs included double-label immunohistology with prosaposin and either phalloidin (labeling the stereocilia and portions of the OHC membrane), synaptophysin (an auditory efferent terminal label), or ChAT (Fig. 3*B–E*). Double labeling prosaposin with phalloidin (Fig. 3*B*) shows that prosaposin is predominantly located below the basilar pole of the OHC. Double labeling with synaptophysin (Fig. 3*C*) also shows that prosaposin is predominantly located at or below the efferent auditory terminal label and in the DCs. Last, triple labeling with ChAT and DAPI (labeling cell nuclei), either in the rat (Fig. 3*D*) or mouse (*E*) also shows that prosaposin localizes below the OHC, in the efferent synaptic cleft and DCs. Together, these studies demonstrate that prosaposin protein (and/or saposin D protein, because the antibody labels both) predominantly exists in the apex of the DCs and the efferent synaptic cleft between the OHCs and DCs.

Because initial RT-PCR studies (Fig. 3*A*) clearly demonstrated prosaposin mRNA in the OHC, at odds with the immunofluorescent labeling studies, additional real-time quantitative RT-PCR was used for additional characterization of prosaposin in OHCs versus DCs (Fig. 3*F*). These quantitative studies, in populations of 200 OHCs and DCs, demonstrate that DCs transcribe a larger amount of prosaposin mRNA than OHCs, although OHCs clearly do make prosaposin mRNA as well. On average, when compared with the ribosomal housekeeping gene L19, there was a 4-fold increase in prosaposin concentration in OHCs and a 6.5-fold increase in DCs. However, in contrast to standard RT-PCR from smaller populations of microdissected OHCs, in the quantitative-PCR experiments, we consistently obtained small amounts of GLAST1 in the OHC preparation (indicative of some DC contamination), whereas we never had α10 contamination in the DC samples (indicating relatively pure populations of DCs), although this level of GLAST1 was not enough to account for the presence of prosaposin mRNA in the OHC samples.

The discrepancy between these immunohistology and RT-PCR studies showing prosaposin mRNA in OHCs but not translated protein might be accounted for by the antibody, which is directed against the c-terminal region of prosaposin, corresponding to the region encoding saposin D. Prosaposin, which itself can be an active protein, is also post-translationally cleaved into one of four saposins, A–D. If the predominant saposin in the OHC was another saposin (such as saposin C), then prosaposin mRNA would be detected in the OHC, whereas immunohistology would

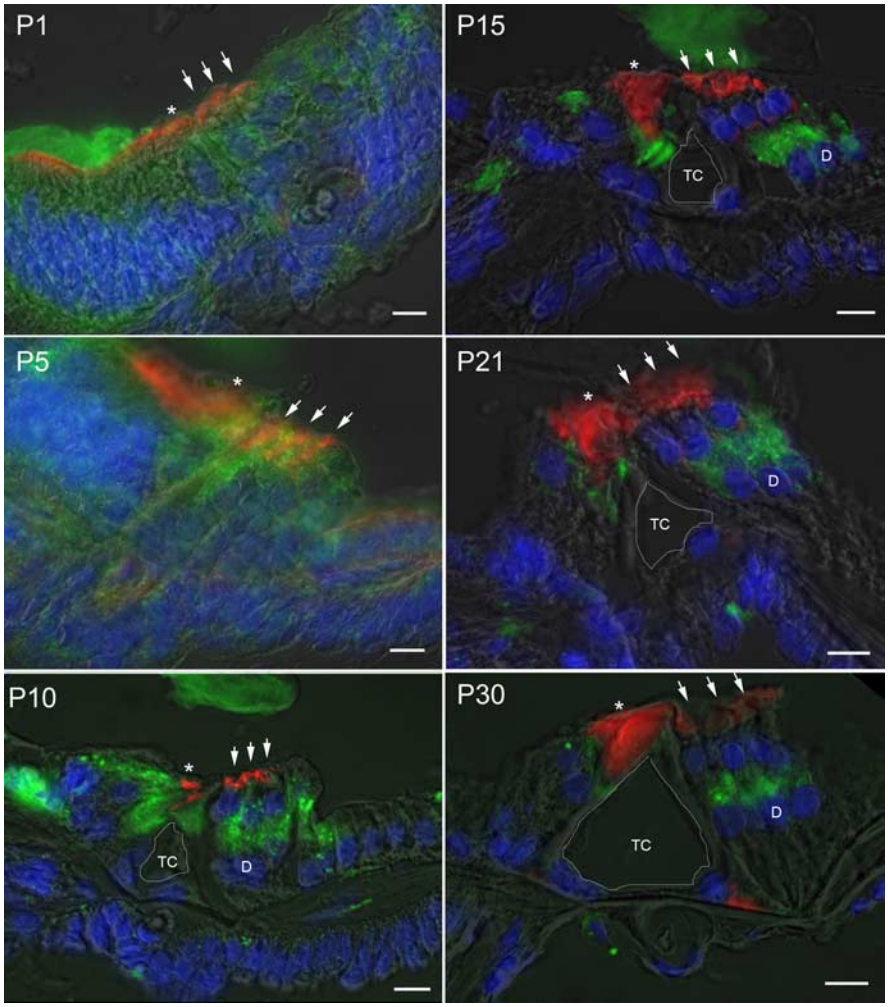

Figure 2. Developmental expression of prosaposin in rat cochlea. Immunofluorescence staining of prosaposin (green), rhodamine-phalloidin (red), and DAPI (blue) with a semitranslucent transmitted light micrograph overlay from P1 through P30 demonstrates initially diffuse expression of prosaposin throughout the primitive organ of Corti that gradually localizes to several discrete locations within the organ of Corti, including the IHCs and its supporting cells, inner pillar cells, and synaptic region of the OHCs (either base of OHCs or apex of the DCs). At P5 there is increased signal in the regions of the IHC and OHC relative to surrounding tissues. By P10, labeling can be clearly differentiated in the region of the basal OHCs or apical DCs, IHCs, and inner pillar cells. This labeling pattern is refined, with further loss of label in surrounding cells through P30, with localization to regions surrounding the IHC, inner pillar cell, and base of OHC and/or apex of DC. In each panel, an asterisk is placed above the IHC, three small arrows are placed above the OHC, and the central of the three Deiters' cells is marked by a D where clearly visible (after P10). The tunnel of Corti is outlined in white and labeled TC. Scale bars, 10 μm.

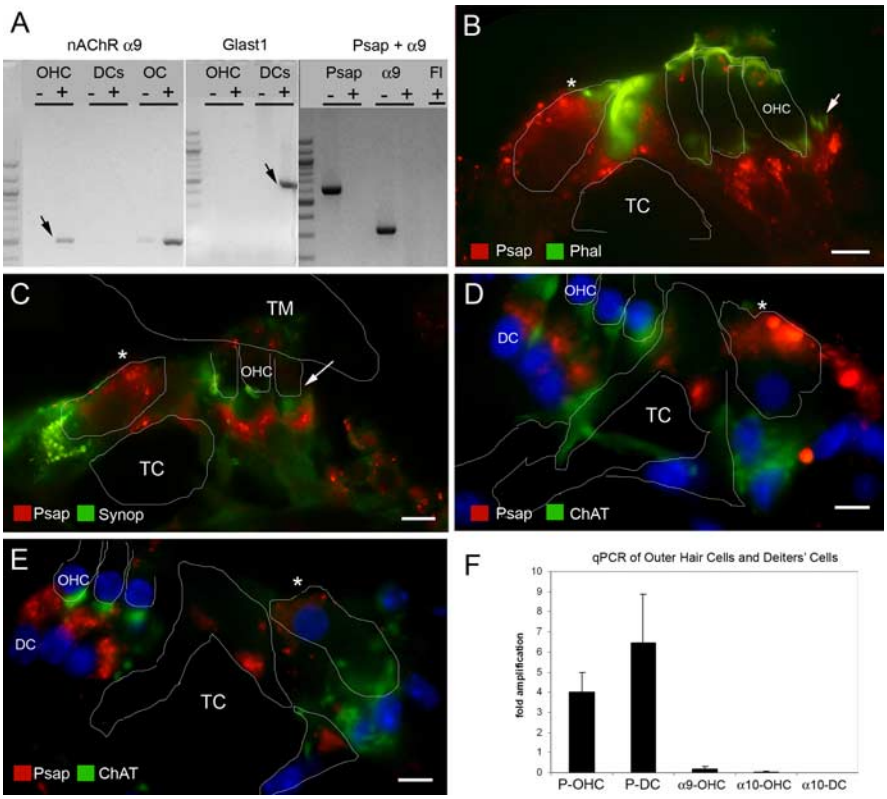

Figure 3. Localization of prosaposin in the organ of Corti by RT-PCR and immunohistology. Multiple modalities were used to localize prosaposin in the region of the OHCs and DCs. ***A***, RT-PCR from microdissected rat OHCs. A first round RT-PCR (left) demonstrates the presence of α9 (arrow; used here as an OHC marker; similar results were obtained with α10) (data not shown) from OHCs, but not DCs. Similarly, a whole section of the organ of Corti (OC) demonstrates a strong band of α9. To verify that DCs have not contaminated the OHC sample, the presence of Glast1 mRNA (arrow; present only in DCs) is tested using two successive rounds of PCR (middle). The right panel demonstrates the presence of both α9 and prosaposin (Psap) in OHCs, but not in the background fluid (FI), clearly indicating the presence of prosaposin mRNA in OHCs. ***B***, Double labeling of rat organ of Corti with prosaposin (red) and phalloidin (Phal, green) demonstrates that prosaposin lies predominantly below the basal region of the OHCs (arrow, outline of OHC base), in the efferent synaptic cleft and/or Deiters' cell. Intense prosaposin labeling is also noted in the IHC region (asterisk). ***C***, Double labeling of rat organ of Corti with prosaposin (red) and synaptophysin (green) demonstrates that prosaposin predominantly lies at or below the efferent synaptic cleft (arrow) below the base of the OHC, again suggesting predominant prosaposin labeling in the apex of the DCs or efferent synaptic cleft. Once again, strong prosaposin labeling is also noted in the IHC (asterisk). TM, Tectorial membrane. ***D***, ***E***, Triple labeling of prosaposin (red), ChAT (green), and DAPI (blue labels nuclei) in either rat (***D***) or mouse (***E***) organ of Corti, demonstrates that prosaposin resides largely in the efferent synaptic cleft and the apex of the DCs. For orientation, the OHCs, pillar cells, and IHC (asterisk) are outlined in white, whereas the tunnel of Corti (TC) is labeled, as are the third OHC and DC nuclei. ***F***, To resolve the discrepancy of the RT-PCR and immunofluorescence results regarding prosaposin in OHCs, quantitative real-time PCR of microdissected OHCs and DCs was performed. Compared with L19, a ribosomal housekeeping gene, prosaposin shows a 4-fold amplification in OHCs (P-OHC) and a 6.5-fold amplification in DCs (P-DC), indicating higher levels of prosaposin mRNA in DCs as compared with OHCs. For comparison, both nAChR α9 and α10 show a marked decrease in concentration as compared with L19 in OHCs (α9-OHC and α10-OHC, respectively). As a control, there is no α10 identified in DCs, indicating a relatively pure population of cells. Together, these studies suggest that prosaposin exists mostly in DCs or the efferent synaptic cleft, whereas the OHCs contains a much smaller concentration of prosaposin. Error bars indicate SEM. Scale bars, 10 μm.

only detect saposin D, and not saposins A–C. Unfortunately, microdissected OHCs do not yield enough protein to perform an adequate Western blot analysis, which might resolve this discrepancy, whereas available saposin C antibodies have not been able to resolve this question (data not shown).

Prosaposin knock-out mice studies

To gain some insight into the possible functional role of prosaposin or saposins A–D within the organ of Corti, prosaposin knock-out mice were studied (Sun et al., 2002). It has previously been demonstrated that both prosaposin and one of its mature, cleaved proteins, saposin C, can cause neuronal outgrowth in cell cultures (O'Brien et al., 1995). The CNS effects of such a mutation have already been described (Sun et al., 2002), however the effects on the auditory pathway and end organ have not been reported. Because the homozygote (−/−) KO mice uniformly expire shortly after P30, all studies were performed before this time. In contrast, the heterozygotes and WT live normally with no apparent functional deficits for at least 1 year.

Initial studies were undertaken to verify the phenotype within these mice. As shown (Fig. 4), homozygote prosaposin KO mice lack prosaposin expression within the organ of Corti (Fig. 4*A*). The immunofluorescence results are similar to those seen in Figure 3*E*. Western blot analysis in the KO mouse also demonstrates a lack of prosaposin expression within the brain, a known location of prosaposin, in contrast to heterozygote and WT mice (Fig. 4*B*). Some bands of unexpected size are seen in the brain samples of each of the mice, including the KO mice and, thus, this likely represents nonspecific binding. These studies also demonstrate that prosaposin expression in the mouse (Fig. 4*A*) is similar to that in the rat (Figs. 2, 3), indicating little, if any variability in prosaposin expression patterns in rodents.

Functional analysis of hearing in KO mice

Hearing in these knock-out mice was tested using standard ABR threshold analysis and DPOAEs. Mice were bred in an FVB background, a strain with minimal auditory deficits. In mice, detectable ABR thresholds are typically not seen until after P14 (Kraus and Aulbach-Kraus, 1981). Mice at varying ages were thus tested through P30 (Fig. 5*A*) using clicks, and at 8, 16, and 32 kHz (Fig. 5*A*,*B*). As shown (Fig. 5*A*), all mice demonstrate normal auditory development through P19, with ABR thresholds being statistically significantly higher in the homozygotes as compares to heterozygotes and WT. After P19, however, hearing in the homozygote KO mice declines rapidly whereas hearing stays normal in the heterozygote and WT mice.

DPOAEs were also obtained from mice at these same ages. Before P19, DPOAE amplitudes are significantly reduced at very low (8 kHz) and high (32 kHz) frequencies for the homozygotes as compared with heterzygotes and WT mice (Fig. 5*C*). By P30, DPOAEs are significantly reduced at all frequencies tested for the KO mice as compared with heterozygotes and WT (Fig. 5*D*).

Cochlear knock-out histology

The inner ears of P12–P30 homozygote KO, heterozygote, and WT mice were analyzed using standard histological analysis (Fig. 6) to gain a better understanding of the effects of such a mutation on inner ear anatomy and to better understand why the homozygote mice rapidly lost hearing after P19. As expected, the WT

mice had normal organ of Corti anatomy (Fig. 6*A*,*C*,*E*,*G*). The heterozygote mice (data not shown) show normal overall cochlear morphology and bony anatomy, but do demonstrate a subtle cellular hyperplasia of the cells lining the region of the inner sulcus and greater epithelial ridge.

In contrast, there were a number of abnormalities identified in the organ of Corti of the homozygote KO mice (Fig. 6*B*,*D*,*F*,*H*). As early as P12 (Fig. 6*A*), there is cellular hypertrophy in the region of the inner hair cell, which continues through P30 (Fig. 6*F*,*H*, black arrows, only shown through P25). By P15, a small bulge of tissue appears in the tunnel of Corti adjacent to the inner pillar cell, which increases in size through P30 (Fig. 6*D*,*H*, red arrows). OHC anatomy also becomes distorted through P30, with hypertrophy of the DCs, and loss of OHCs at the cochlear apex (see below). There is also increasing hypertrophy of the cells lining the inner sulcus. Otherwise, the inner ear appears normal, with intact Reisner's membrane, stria vascularis, spiral ganglion, and cochlear scalae.

These changes appear even more striking in electron micrographs (Fig. 7). As compared with WT (Fig. 7*A*), the KO mice show marked cellular hypertrophy in the region of the IHC (Fig. 7*B*,*C*), bulging tissue into the tunnel of Corti (Fig. 7*B*,*C*,*E*), and hypertrophy of the inner sulcus region (Fig. 7*D*). In the region of the OHCs, DCs are hypertrophied (Fig. 7*F*) and there is vacuolization within the OHCs (Fig. 7*F*–*H*). The synaptic cleft between the OHC and the DCs is also abnormally enlarged (Fig. 7*H*).

Initial studies demonstrated loss of OHCs at the cochlear apex and, thus, cytocochleograms were obtained for both IHCs and OHCs (Fig. 8). Compared with WT mice, there is a loss of up to 40% of OHCs in the cochlear apex of the prosaposin KO mice, extending through the first 2 mm of the cochlear duct. In contrast, IHC numbers are normal throughout the cochlea.

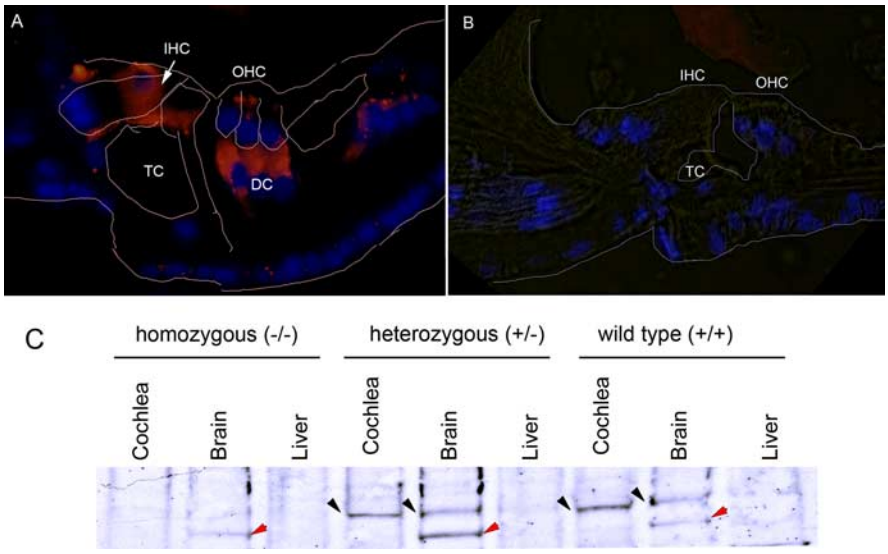

Figure 4. Prosaposin expression in the null mutant (knock-out) mouse. Prosaposin antibody labeling demonstrates the absence of prosaposin in the KO mouse organ of Corti. ***A***, ***B***, Compared with WT mice (***A***), homozygote prosaposin KO mice lack prosaposin expression within the organ of Corti (***B***). TC, Tunnel of Corti. ***C***, In the homozygous (KO) mice, Western blot analysis demonstrates a lack of prosaposin expression within the brain, a known location of prosaposin, in contrast to heterozygote and WT mice (black arrow). In all three brain lanes, there is nonspecific banding (red arrows); because the band also appears in the KO sample, it is not prosaposin labeling. The nonspecific band does not appear in the cochlear samples, and, thus, the labeling seen in the cochlea likely represents true prosaposin labeling. The brain serves as a positive control whereas the liver serves as a negative control in each experiment.

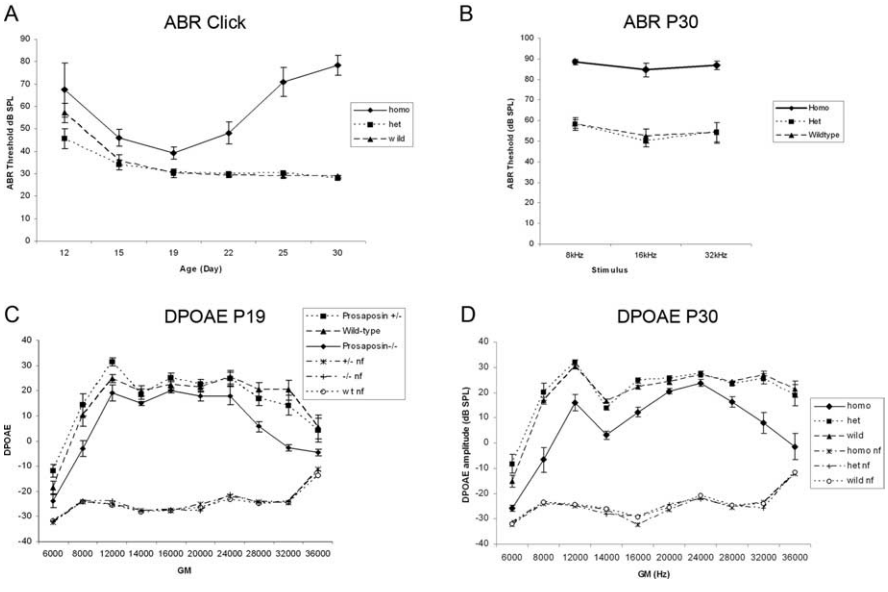

Figure 5. Hearing in the prosaposin knock-out mice. ***A***, ***B***, Mice at varying ages were tested through P30 (***A***) using clicks, and at 8, 16, and 32 kHz (***B***). ***A***, All mice demonstrate normal auditory development through P19, although ABR thresholds are statistically significantly higher in the homozygotes as compared with heterozygotes and WT. After P19, however, hearing in the homozygote KO mice declines rapidly whereas hearing stays normal in the heterozygote and WT mice. ***C***, DPOAEs were obtained from mice at these same ages. Before P19, DPOAE amplitudes are significantly reduced at very low (8 kHz) and high (32 kHz) frequencies for the homozygotes as compared with heterzygotes and WT mice. ***D***, By P30, DPOAEs are significantly reduced at all frequencies tested for the KO mice as compared with heterozygotes and WT. nf, Noise floor.

Immunofluorescent histology of knock-out mice

To gain a greater insight into the nature of the histologic changes seen in the organ of Corti in the KO mice, immunofluorescence using antibodies toward synaptophysin, which labels efferent auditory fibers (Schimmang et al., 2003), and NF-200, which labels afferent auditory fibers (Berglund and Ryugo, 1991), was undertaken (Fig. 9). Histologic sections were analyzed from mice at P11, when the auditory system was functionally immature, and at P21, a time at which the heterozygote and WT mice had measurable ABR thresholds, but by when the KO mice had lost a significant amount of hearing.

At P11 (Fig. 9*A*), NF-200 demonstrated normal labeling in the wild-type and heterozygote mice, with signal in the region of the inner hair cells and along the afferent projections to the spiral ganglion (Wiechers et al., 1999). In contrast, there was barely a

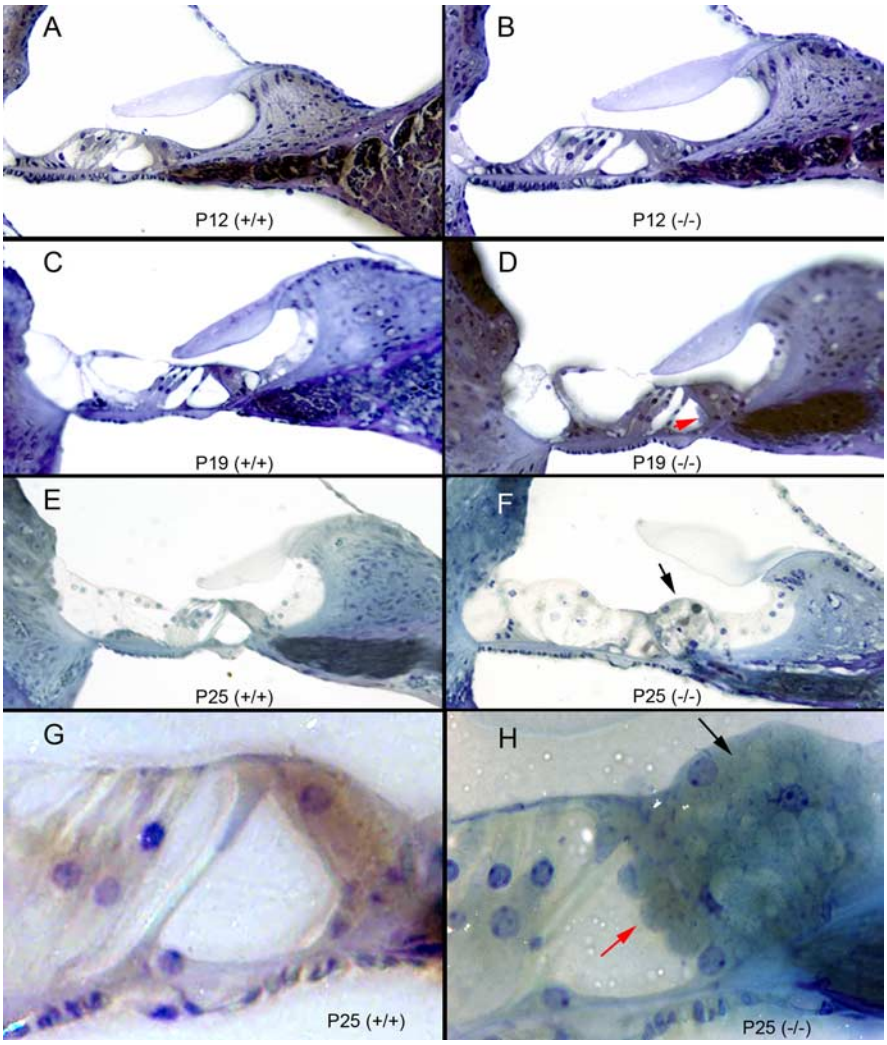

Figure 6. Cochlear histology in the prosaposin knock-out mice; mouse organ of Corti histology when the neuritogenic region of saposin C is mutated to become nonfunctional. ***A***, ***C***, ***E***, ***G***, Normal P12, P19, and P25 (low and high magnification) wild-type (+/+) mouse organ of Corti histology (***A***, ***C***, ***E***, 40× magnification; ***G***, 100× magnification). ***B***, ***D***, ***F***, ***H***, The homozygous (−/−) mouse organ of Corti at varying ages (P12, P19, and P25 at low and high magnification). The gross morphology (e.g., number of turns) is identical to the wild-type, as is the spiral ganglion cell number and cellular morphology. Beginning at P15 and increasing through P30, there is marked hyperplasia of cells surrounding the inner hair cell and in the region of the inner sulcus and greater epithelial (***F***, ***H***, black arrow highlights this change). There is also some tissue bulging into the tunnel of Corti from the inner hair cell region, noted as early as P15, and here labeled at P19 and P25 (***D***, ***H***, red arrows). DCs also appear larger than normal with an ill-defined border between the DCs and the OHCs in animals beyond P25 (most notable in ***F***).

perceptible staining pattern in the homozgote KO mice at this same age (Fig. 9*B*). By P21 however (Fig. 9*C*,*D*), the mutant mice developed an intense NF-200 staining pattern in the region corresponding to the cellular proliferation surrounding the inner hair cell that was seen on light and electron microscopy, indicating an exuberant growth of afferent terminals surrounding the IHCs. This staining pattern suggests a delay in the development of afferent terminals in the KO mice initially (at P11), with subsequent prolific sprouting by P21.

Synaptophysin has a slightly different staining pattern in the mutant mice (Fig. 9*E–H*). Again, the WT and heterozygote mice had identical and predicted staining patterns, with labeling in the regions of the IHCs and OHCs (Knipper et al., 1995). At P11 (Fig. 9*F*), the homozygous KO mice demonstrate slightly decreased staining intensity in the region of the inner hair cells, and little to no staining in the region of the OHCs. By P21 (Fig. 9*H*), the homozygote KO mice show a small amount of signal in the region of the OHCs, and an intense staining pattern in the region of the tunnel of Corti, precisely correlating with tissue bulge into the tunnel of Corti seen in the light and electron micrograph sections (compare Figs. 6*F*,*H*, 7*B–C*,*E*). This staining pattern strongly suggests that the tissue bulging into the tunnel of Corti represents a proliferation of efferent nerve terminal endings attempting to cross the tunnel of Corti on their way to the OHCs. It should be noted that the staining does not allow differentiation between medial efferents (which synapse onto IHCs during development, but are subsequently lost, and synapse later onto OHCs) and lateral efferents (which synapse onto the afferent dendrites of the IHCs).

Hair cell electrophysiology

Functional effects on innervation were examined by whole-cell voltage-clamp recordings from hair cells in the excised organ of Corti of heterozygous and homozygous prosaposin deficient mice. However, despite repeated attempts, no adequate recordings could be obtained from OHCs in the homozygous organ of Corti. In the few whole-cell recordings that were achieved, large leak currents were found, and active membrane currents were poor or absent. These results are likely to be related to the OHC histopathology observed with electron microscopy and justified the conclusion that assessment of cholinergic function in these cells would not be reliable. Then, as an alternative, we took advantage of the transient efferent synapses formed on IHCs in the first two postnatal weeks (Katz et al., 2004). Thus, we recorded current-voltage *I–V* relationships from IHCs before the onset of hearing (P7–P11) and at ~3 weeks of age (P19) (Fig. 10). The *I–V* relationships of prosaposin heterozygous (+/−) and homozygous (−/−) mice did not exhibit any obvious changes compared with (+/+) mice: at P7–P11, IHC *I–V* relationships showed Ca^{2+} inward currents and delayed rectifier potassium currents for WT (six IHCs), heterozygote (+/−) (six IHCs), and homozygote mutant (−/−) mice (three IHCs) (Fig. 7*A*). At P19, homozygote (−/−) IHC *I–V* relationships exhibited the usual substantial large conductance potassium channel (BK channel) potassium current that appears after the onset of hearing, which can be identified by its fast activation time compared with the slower activation time of delayed rectifier potassium currents [homozygote (−/−); three IHCs] (Fig. 10*B*). In mouse IHCs, BK potassium currents start to be expressed around the onset of hearing (P14) (Kros et al., 1998).

We next examined cholinergic synaptic function in prosaposin (−/−) mice. In wild-type animals, IHCs receive direct cholinergic efferent input from the medial efferent neurons during the first two postnatal weeks. Cholinergic innervation is lost from

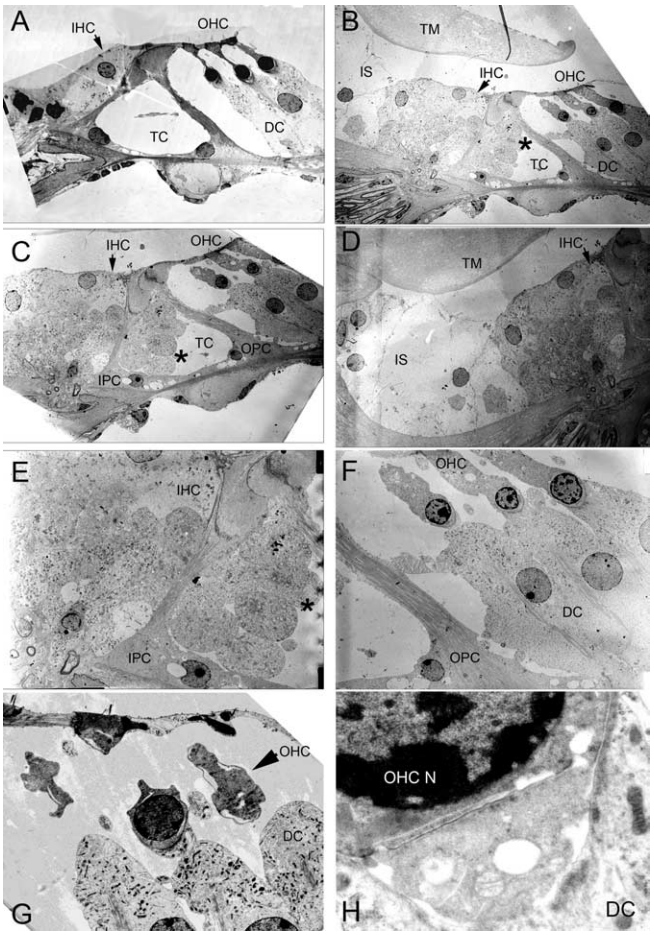

Figure 7. Cochlear electron microscopy of the prosaposin knock-out mice. ***A***, Wild-type organ of Corti demonstrating normal anatomy. ***B***, ***C***, In the prosaposin KO mouse, there is marked cellular hypertrophy in the region of the IHCs. ***B***, ***C***, ***E***, There is bulging tissue into the tunnel of Corti (TC, asterisk). ***D***, Hypertrophy of the inner sulcus (IS) region. ***F–H***, In the region of the OHCs, DCs are hypertrophied and there is vacuolization within the OHCs. ***H***, The base of the OHC, efferent synaptic cleft, and apex of the DC. The synaptic cleft between the OHC and the DCs is abnormally enlarged and vacuolization is seen in the cells. TM, Tectorial membrane; OPC, outer pillar cell.

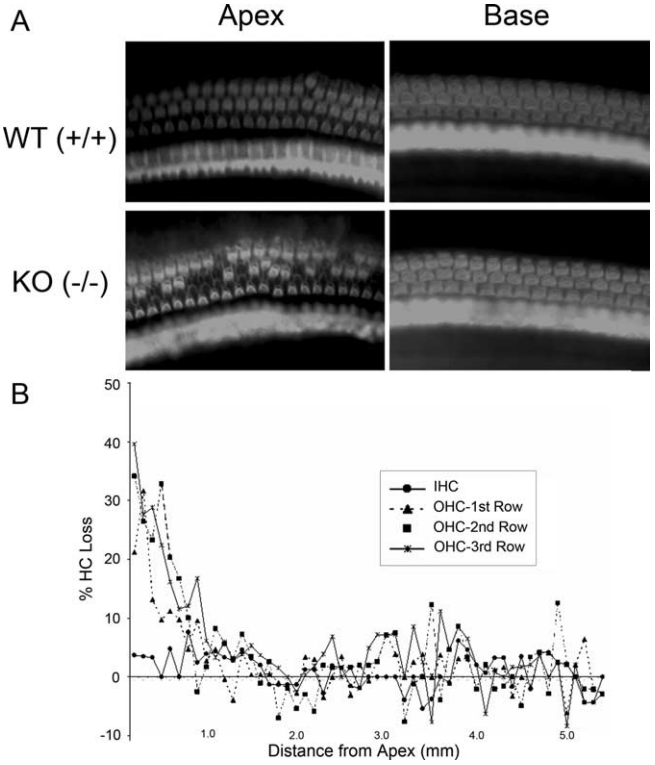

Figure 8. Hair cell counts in the prosaposin knock-out mice. ***A***, Representative samples of phalloidin-stained cochlear preparations in the base and apex of WT and KO mice. There is a loss of OHCs in the apex of the KO mice. ***B***, Hair cell cytocochleogram in the organ of Corti. Compared with WT mice, there is a loss of up to 40% of OHCs in the cochlear apex of the prosaposin KO mice, extending through the first 2 mm of the cochlear duct. In contrast, IHC numbers are normal throughout the cochlea.

IHCs after the onset of hearing, but maintained in the OHCs (Simmons, 2002). This is seen as the loss of response to exogenous ACh and efferent synaptic currents in IHCs after the onset of hearing (Katz et al., 2004).

We tested IHCs for ACh-activated currents and also for efferent synaptic activity in cochleae before and after the onset of hearing: at age P7–P11 we found ACh-activated currents and efferent synaptic currents in IHCs from wild-type mice (six of six IHCs), prosaposin (+/−) mice (six of six IHCs), and also prosaposin (−/−) mice (Fig. 10*C*) (three of three IHCs). The ACh-activated currents (100 μM ACh) were inward at a holding potential of −90 mV and outward at −50 mV, suggesting, that both ACh receptors and SK current were functional. In all animals tested, including the prosaposin (−/−) mice, application of 25 mM potassium induced an inward current caused by the change in the potassium reversal potential in IHCs, and also activated synaptic activity (Fig. 10*E*). At age P19, prosaposin (−/−) mice showed the normal developmental loss of cholinergic sensitivity: application of ACh did not elicit any currents (Fig. 10*D*). Application of 25 (or 40) mM potassium induced an inward current, but did not activate any efferent synaptic activity (three of three IHCs) (Fig. 10*F*). In summary, in prosaposin (−/−) mice, the efferent fibers contacting IHCs behave as those found in the wild-type. Before the onset of hearing, efferent synapses mediate cholinergic synaptic activity, and after the onset of hearing, efferent synaptic function and sensitivity to ACh is lost at the IHC.

Discussion

This work identified a here-to-fore unknown cochlear gene product, prosaposin, from a yeast two-hybrid screen using the hair cell nAChR subunit α10 as bait. Prosaposin knock-out mice became deaf, suffered a loss of OHCs in the cochlear apex, and had striking abnormalities of neuronal innervation. These results suggest that prosaposin, and/or one of its mature cleaved end-products, saposins A–D, is involved in the maintenance of normal neural connectivity within the mammalian organ of Corti.

A question remains, however, whether there is a true physiologic interaction between nAChR subunit α10 and prosaposin in the ear. Findings suggestive of a prosaposin–α10 interaction include the fact that prosaposin was identified through a yeast two-hybrid protein–protein binding assay using α10, the overlapping distribution of prosaposin and α10 mRNA in outer hair cells, prosaposin immunoreactivity in the adjacent synaptic cleft and apical Deiters' cells, and a loss of apical OHCs and reduced DPOAEs in the prosaposin KO mice, implying an efferent, OHC effect. In contrast, factors suggesting an alternate role for prosaposin in hearing not related to α10 function include the broader expression pattern of prosaposin beyond hair cells including Deiters' cells and the unusual neural morphology of KO mice that is

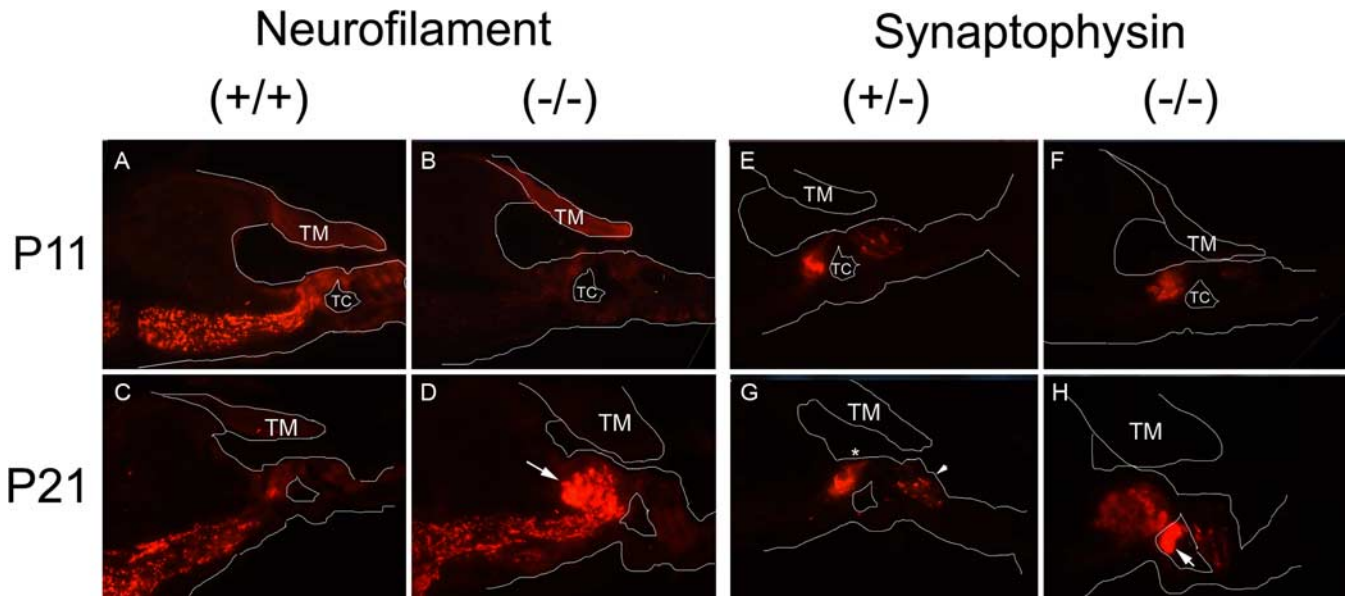

Figure 9. Cochlear immunohistochemistry of the prosaposin knock-out mice. Immunofluorescent labeling with neurofilament and synaptophysin antibodies in the knock-out mice organ of Corti lacking a functional neuritogenic region of saposin C. A white outline of relevant structures within the organ of Corti are added within each picture to orient the staining pattern. ***A–D***, Neurofilament-200 (afferent auditory neuronal) staining at both P11 (***A***, ***B***) and P21 (***C***, ***D***). The staining pattern shows intense labeling at P11 in the wild-type (identical to the heterozygote) (data not shown), but weak labeling in the homozygote by comparison. By P21, the heterozygote has a normal amount of labeling, whereas the homozygote has an abundance of labeling in the region corresponding the hypercellular region surrounding the inner hair cell seen in Figures 6 and 7. ***E–H***, Synaptophysin (efferent auditory neuronal) staining at P11 (***E***, ***F***) and P21 (***G***, ***H***). At P11, there is very little difference between wild-type (data not shown), heterozygous (***E***) and homozygous (***F***) knock-out mice organ of Corti. By P21, in the WT (data not shown) and heterozygote (***G***), staining is noted in the region of the IHC (below asterisk) and base of the OHCs (small arrow), as expected. In contrast, in the KO mice (***H***), there is a significant amount of synaptophysin staining in the regions of the tunnel of Corti (TC; arrow) and to a lesser extent, the region surrounding the IHC. There is limited staining noted in the region of the OHCs in both P11 and P21 homozygotes as compared with heterozygotes or WT at both ages. The cellular bulging into the tunnel of Corti seen in Figure 6 and 7 corresponds exactly to the intense synaptophysin staining here in the homozygote (***H***). TM, Tectorial membrane.

quite different from the described α10 KO mouse (Murthy and Vetter, 2006).

Although not reported previously, it is reasonable to surmise that there are protein–protein interactions involving the intracellular loops of the nAChR α9α10 within OHCs. For example, the intracellular loop of the nAChR subunit α4 has been shown to directly bind to the chaperone protein 14–3-3eta to assist with subunit stabilization, as well as the calcium sensor protein visinin-like protein-1, thought to modulate the surface expression and agonist sensitivity of the α4β2 nAChR (Jeanclos et al., 2001; Lin et al., 2002).

Prosaposin, a precursor of saposins A–D, is a multifunctional protein that has both intracellular and extracellular functions, most notably stimulating the hydrolysis of a number of sphingolipids (Kishimoto et al., 1992). Mutations in saposin C have been linked to lysosomal storage diseases such as Gaucher's disease (Horowitz and Zimran, 1994). Additionally, prosaposin and saposin C can act as neurotrophic factors in culture, bind to a putative G_0-coupled cell surface receptor, and may be involved in the prevention of cell death (O'Brien et al., 1994; Hiraiwa et al., 1997; Campana et al., 2000; Misasi et al., 2004). The region responsible for this "neuritogenic" effect is a 22 amino acid region within saposin C (Qi et al., 1996). There is evidence that saposin D acts as an acid ceramidase inhibitor, whereas mice deficient in saposin D demonstrate renal pathology, imbalance, and loss of cerebellar Purkinje cells (Matsuda et al., 2004).

The aberrant hypertrophy of auditory efferent and afferent fibers in the KO mice may be a result of failed path-finding or innervation normally supported by prosaposin or saposins A–D. This suggests that feedback signals that normally terminate auditory afferent and efferent outgrowth fail in the prosaposin KO. The prosaposin KO mice demonstrate a trend toward normal hearing development through P19, but rapidly lose hearing after this (Fig. 5), suggesting that the consequences of altered innervation appear to be gradual, presumably relating to the progressive degeneration and loss of OHCs in the knock-outs. In addition to a loss of the "cochlear amplifier" provided by OHC electromotility, it is possible that afferent activity is reduced or desynchronized, consistent with central neuronal demyelination and degeneration also found in the prosaposin knock-out (Sun et al., 2002). Again, whether these changes are related to an interaction between prosaposin and α10 is unclear.

The substantial structural and functional changes seen in the prosaposin KO mice leave the IHCs relatively unscathed, and voltage-clamp recordings revealed no obvious defects of IHC electrophysiology. In particular, cholinergic sensitivity and synaptic activity appeared normal, and disappeared on schedule after the onset of hearing, as in WT mice. Furthermore, the usual developmental changes in excitability caused by the postnatal acquisition of large-conductance, BK potassium channels (Kros et al., 1998) also occurred in the knock-out IHCs. In contrast, even by P19 the knock-out OHCs were sufficiently damaged so that the patch-clamp recording was not possible, and apical OHCs, but not IHCs degenerate and disappear from the knock-out cochleae. Thus, a deficit in prosaposin preferentially targets the OHCs, perhaps relating to the markedly aberrant efferent outgrowth.

Although the present work shows a number of potential connections between prosaposin and α10, genetic deletion of the nAChR subunit itself does not produce identical effects. In particular, the loss of α10 does not cause hearing loss, OHCs do not degenerate, and efferent nerve fibers find their way across the tunnel of Corti to make contacts on the base of OHCs (Murthy and Vetter, 2006). One possible related observation is that only

single, hypertrophic efferent endings were found on the α10 knock-out OHCs, compared with multiple smaller endings in wild-type mice. Similar results were observed for the α9 knock-out mouse (Vetter et al., 1999). These observations reinforce the present conclusion that prosaposin or one of its cleaved products is specifically required for competent cochlear neuronal pathfinding, but may mediating these effects independent of the hair cell AChR.

One important question to ask is why we see binding between nAChR α10 and prosaposin, but not α9? Current evidence suggests that α9 expression in hair cells occurs before synaptogenesis, whereas α10 expression is concomitant with the presence of efferent fibers (Simmons and Morley, 1998; Simmons, 2002). It is thus possible that this correlation relates to the protein–protein interaction we have identified between prosaposin and α10, and suggests an additional role for α10 along with prosaposin in establishment of neural connections. The location of the receptor subunit at the base of the hair cell would make α10 an ideal target for an innervating efferent neuron at a critical time during the development of hearing. Because of the tight regulation required for normal auditory system development, it would make sense that a feedback signal must be provided to "turn off" further neuronal growth when the target cell has been innervated. Perhaps prosaposin, through its interaction with α10, helps provide such feedback, explaining the proliferation of efferent fibers within the tunnel of Corti. Both saposin C and prosaposin can act as neurotrophic factors *in vivo* and *in vitro* (Campana et al., 2000), which is why the findings of neurite sprouting in this KO mouse, lacking prosaposin function, are surprising. However, the present results imply that efferent, and possibly afferent auditory fibers undergo unchecked growth in the absence of the usual "targeting" signal that prosaposin provides.

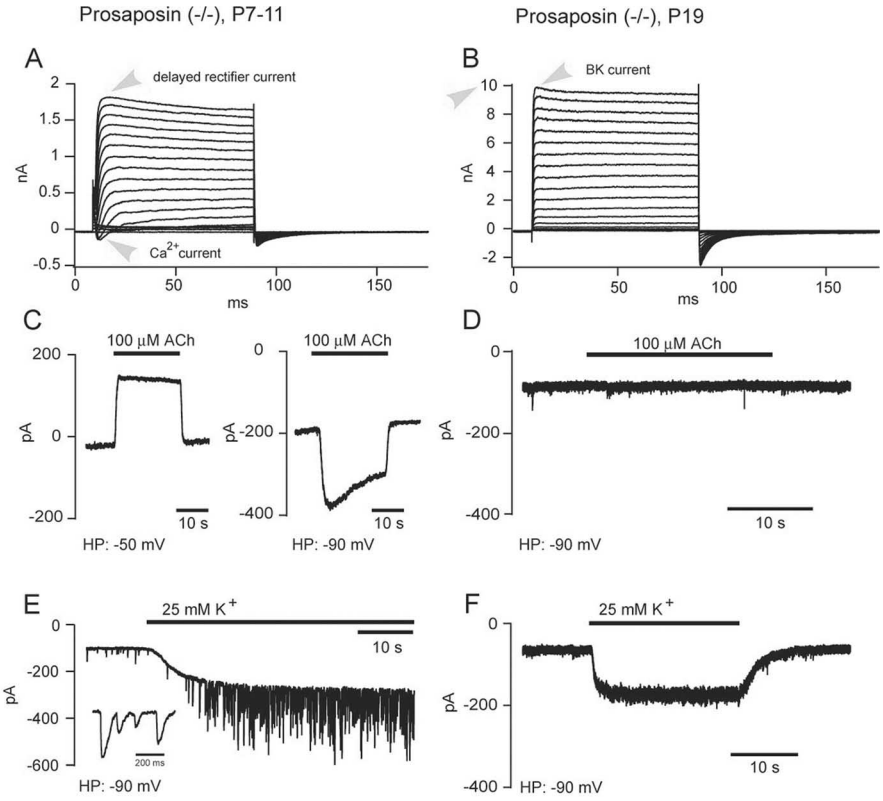

Figure 10. Hair cell physiology in the prosaposin knock-out mice. Cholinergic efferent synapses at the IHC show normal function in prosaposin (−/−) mice. Animals were tested before (P7–P11) and after (P19) the onset of hearing. ***A***, ***B***, At P7–P11, IHC *I–V* relationships showed Ca^{2+} inward currents and delayed rectifier potassium currents. At P19, IHC *I–V* relationships also exhibited substantial BK potassium currents, which can be identified by a fast activation time compared with the slower activation time of delayed rectifier potassium currents. ***C***, ***E***, At age P7–P11, prosaposin (−/−) mice, like the wild-type, exhibited ACh-activated currents and efferent synaptic currents in IHCs. The ACh-activated (100 μM) currents were inward at a holding potential of −90 mV and outward at −50 mV, suggesting that both ACh receptors and SK current were functional. Application of 25 mM potassium induced an inward current in IHCs, and also activated synaptic activity. ***D***, ***F***, At age P19, prosaposin (−/−) mice showed a phenotype as expected for a normal development for efferent innervation: application of ACh did not elicit any currents. Application of 25 (or 40) mM potassium induced an inward current caused by the change in the potassium reversal potential but did not activate any efferent synaptic activity.

The precise nature of how prosaposin would interact with α10 to mediate such developmental feedback is unclear. Because it is the intracellular loop of α10 that contains the binding region, prosaposin must either be made within the hair cell in response to an extracellular signal or, alternatively, secreted by the innervating neuron and taken up secondarily by the hair cell. Either supposition is possible because prosaposin has been described both as a neuronal surface protein as well as an excreted protein (Hineno et al., 1991; Fu et al., 1994). Furthermore, prosaptide, a synthetic peptide comprising the neuritogenic region of saposin C, is active in solution as a neurotrophic factor and can help prevent neurotoxicity (Campana et al., 1998; Lu et al., 2000), signifying that prosaposin may have the ability to modulate cells exogenously. Thus, the predominant presence of prosaposin within the DC and synaptic cleft, directly adjacent to the OHC nAChR, would not necessarily contradict this role. Furthermore, it is possible that saposins A–C may be the active form in the OHC, not detected by our antibody directed against saposin D (prosaposin mRNA was clearly detected within OHC). Because saposin C has been implicated as having neurotrophic properties (O'Brien et al., 1994), it would be an obvious candidate for this role, in addition to the neuronal pathfinding alterations seen here. A transgenic mouse lacking only the neuritogenic region of saposin C had been developed (Sun et al., 2002), but unfortunately no longer exists to test the supposition that this region may be responsible for the changes seen in the prosaposin KO mouse.

Last, the findings in this study might have important potential clinical applications. There is currently a concerted effort by a number of investigators to find ways to improve neuronal survival for profoundly deaf patients who are cochlear implant candidates, because improved neuronal survival would theoretically improve cochlear implant performance (Gao, 1998; Marzella and Clark, 1999; Shepherd and Hardie, 2001; Nakaizumi et al., 2004). If the molecular mechanism of afferent and efferent neuronal proliferation identified in this study can be teased apart and focally applied to the inner ear of profoundly deaf patients, it is possible that increased growth of afferent neurons could translate into improved performance with the cochlear implant. Further-

more, through such a pharmacologic approach, it may also be possible to repair efferent neuronal damage after loud noise exposure or ototoxic insult.

References

Baker ER, Zwart R, Sher E, Millar NS (2004) Pharmacological properties of α9α10 nicotinic acetylcholine receptors revealed by heterologous expression of subunit chimeras. Mol Pharmacol 65:453–460.

Berglund AM, Ryugo DK (1991) Neurofilament antibodies and spiral ganglion neurons of the mammalian cochlea. J Comp Neurol 306:393–408.

Campana WM, Eskeland N, Calcutt NA, Misasi R, Myers RR, O'Brien JS (1998) Prosaptide prevents paclitaxel neurotoxicity. Neurotoxicology 19:237–244.

Campana WM, Mohiuddin L, Misasi R, O'Brien JS, Calcutt NA (2000) Prosaposin-derived peptides enhanced sprouting of sensory neurons in vitro and induced sprouting at motor endplates in vivo. J Peripher Nerv Syst 5:126–130.

Elgoyhen AB, Johnson DS, Boulter J, Vetter DE, Heinemann S (1994) α9: an acetylcholine receptor with novel pharmacological properties expressed in rat cochlear hair cells. Cell 79:705–715.

Elgoyhen AB, Vetter DE, Katz E, Rothlin CV, Heinemann SF, Boulter J (2001) α10: a determinant of nicotinic cholinergic receptor function in mammalian vestibular and cochlear mechanosensory hair cells. Proc Natl Acad Sci USA 98:3501–3506.

Evans MG, Lagostena L, Darbon P, Mammano F (2000) Cholinergic control of membrane conductance and intracellular free Ca^{2+} in outer hair cells of the guinea pig cochlea. Cell Calcium 28:195–203.

Eybalin M (1993) Neurotransmitters and neuromodulators of the mammalian cochlea. Physiol Rev 73:309–373.

Flock A, Russell I (1976) Inhibition by efferent nerve fibres: action on hair cells and afferent synaptic transmission in the lateral line canal organ of the burbot Lota lota. J Physiol (Lond) 257:45–62.

Fu Q, Carson GS, Hiraiwa M, Grafe M, Kishimoto Y, O'Brien JS (1994) Occurrence of prosaposin as a neuronal surface membrane component. J Mol Neurosci 5:59–67.

Fuchs PA, Murrow BW (1992a) Cholinergic inhibition of short (outer) hair cells of the chick's cochlea. J Neurosci 12:800–809.

Fuchs PA, Murrow BW (1992b) A novel cholinergic receptor mediates inhibition of chick cochlear hair cells. Proc R Soc Lond B Biol Sci 248:35–40.

Furness DN, Hulme JA, Lawton DM, Hackney CM (2002) Distribution of the glutamate/aspartate transporter GLAST in relation to the afferent synapses of outer hair cells in the guinea pig cochlea. J Assoc Res Otolaryngol 3:234–247.

Galambos R (1956) Supression of auditory nerve fibers by stimulation of efferent fibers to the cochlea. J Neurophysiol 19:424–437.

Galzi J, Revah F, Bessis A, Changeux JP (1991) Functional architecture of the nicotinic acetylcholine receptor: from electric organ to brain. Annu Rev Pharmacol 31:37–72.

Gao WQ (1998) Therapeutic potential of neurotrophins for treatment of hearing loss. Mol Neurobiol 17:17–31.

Hineno T, Sano A, Kondoh K, Ueno S, Kakimoto Y, Yoshida K (1991) Secretion of sphingolipid hydrolase activator precursor, prosaposin. Biochem Biophys Res Commun 176:668–674.

Hiraiwa M, Campana WM, Martin BM, O'Brien JS (1997) Prosaposin receptor: evidence for a G-protein-associated receptor. Biochem Biophys Res Commun 240:415–418.

Horowitz M, Zimran A (1994) Mutations causing Gaucher disease. Hum Mutat 3:1–11.

Jeanclos EM, Lin L, Treuil MW, Rao J, DeCoster MA, Anand R (2001) The chaperone protein 14–3-3eta interacts with the nicotinic acetylcholine receptor alpha 4 subunit. Evidence for a dynamic role in subunit stabilization. J Biol Chem 276:28281–28290.

Katz E, Elgoyhen AB, Gomez-Casati ME, Knipper M, Vetter DE, Fuchs PA, Glowatzki E (2004) Developmental regulation of nicotinic synapses on cochlear inner hair cells. J Neurosci 24:7814–7820.

Kishimoto Y, Hiraiwa M, O'Brien JS (1992) Saposins: structure, function, distribution, and molecular genetics. J Lipid Res 33:1255–1267.

Klinke R, Galley N (1974) Efferent innervation of vestibular and auditory receptors. Physiol Rev 54:316–357.

Knipper M, Zimmermann U, Rohbock K, Kopschall I, Zenner HP (1995) Synaptophysin and GAP-43 proteins in efferent fibers of the inner ear during postnatal development. Brain Res Dev Brain Res 89:73–86.

Kraus HJ, Aulbach-Kraus K (1981) Morphological changes in the cochlea of the mouse after the onset of hearing. Hear Res 4:89–102.

Kros CJ, Ruppersberg JP, Rusch A (1998) Expression of a potassium current in inner hair cells during development of hearing in mice. Nature 394:281–284.

Leonova T, Qi X, Bencosme A, Ponce E, Sun Y, Grabowski GA (1996) Proteolytic processing patterns of prosaposin in insect and mammalian cells. J Biol Chem 271:17312–17320.

Lin L, Jeanclos EM, Treuil M, Braunewell KH, Gundelfinger ED, Anand R (2002) The calcium sensor protein visinin-like protein-1 modulates the surface expression and agonist sensitivity of the alpha 4beta 2 nicotinic acetylcholine receptor. J Biol Chem 277:41872–41878.

Lioudyno M, Hiel H, Kong JH, Katz E, Waldman E, Parameshwaran-Iyer S, Glowatzki E, Fuchs PA (2004) A "synaptoplasmic cistern" mediates rapid inhibition of cochlear hair cells. J Neurosci 24:11160–11164.

Lu AG, Otero DA, Hiraiwa M, O'Brien JS (2000) Neuroprotective effect of retro-inverso Prosaptide D5 on focal cerebral ischemia in rat. NeuroReport 11:1791–1794.

Lustig LR, Peng H, Hiel H, Yamamoto T, Fuchs PA (2001) Molecular cloning and mapping of the human nicotinic acetylcholine receptor alpha10 (CHRNA10). Genomics 73:272–283.

Martin AR, Fuchs PA (1992) The dependence of calcium-activated potassium currents on membrane potential. Proc R Soc Lond B Biol Sci 250:71–76.

Marzella PL, Clark GM (1999) Growth factors, auditory neurones and cochlear implants: a review. Acta Otolaryngol 119:407–412.

Matsuda J, Kido M, Tadano-Aritomi K, Ishizuka I, Tominaga K, Toida K, Takeda E, Suzuki K, Kuroda Y (2004) Mutation in saposin D domain of sphingolipid activator protein gene causes urinary system defects and cerebellar Purkinje cell degeneration with accumulation of hydroxy fatty acid-containing ceramide in mouse. Hum Mol Genet 13:2709–2723.

McNabb DS, Guarente L (1996) Genetic and biochemical probes for protein-protein interactions. Curr Opin Biotechnol 7:554–559.

Misasi R, Garofalo T, Di Marzio L, Mattei V, Gizzi C, Hiraiwa M, Pavan A, Grazia Cifone M, Sorice M (2004) Prosaposin: a new player in cell death prevention of U937 monocytic cells. Exp Cell Res 298:38–47.

Murthy V, Vetter D (2006) Regulation of olivocochlear innervation and synaptogenesis by cochlear hair cell nicotinic acetylcholine receptors. Paper presented at the Association for Research in Otolaryngology Annual Symposium, Baltimore, MD, February.

Nakaizumi T, Kawamoto K, Minoda R, Raphael Y (2004) Adenovirus-mediated expression of brain-derived neurotrophic factor protects spiral ganglion neurons from ototoxic damage. Audiol Neurootol 9:135–143.

Niedzielski AS, Schacht J (1992) P2 purinoceptors stimulate inositol phosphate release in the organ of Corti. NeuroReport 3:273–275.

O'Brien JS, Kretz KA, Dewji N, Wenger DA, Esch F, Fluharty AL (1988) Coding of two sphingolipid activator proteins (SAP-1 and SAP-2) by same genetic locus. Science 241:1098–1101.

O'Brien JS, Carson GS, Seo HC, Hiraiwa M, Kishimoto Y (1994) Identification of prosaposin as a neurotrophic factor. Proc Natl Acad Sci USA 91:9593–9596.

O'Brien JS, Carson GS, Seo HC, Hiraiwa M, Weiler S, Tomich JM, Barranger JA, Kahn M, Azuma N, Kishimoto Y (1995) Identification of the neurotrophic factor sequence of prosaposin. FASEB J 9:681–685.

Ogawa K, McLaren J, Schacht J (1994) Effect of aging on myo-inositol and phosphoinositide metabolism in the cochlear and vestibular sensory epithelia of the rat. Hear Res 73:155–162.

Qi X, Qin W, Sun Y, Kondoh K, Grabowski GA (1996) Functional organization of saposin C. Definition of the neurotrophic and acid beta-glucosidase activation regions. J Biol Chem 271:6874–6880.

Schimmang T, Tan J, Muller M, Zimmermann U, Rohbock K, Kopschall I, Limberger A, Minichiello L, Knipper M (2003) Lack of Bdnf and TrkB signalling in the postnatal cochlea leads to a spatial reshaping of innervation along the tonotopic axis and hearing loss. Development 130:4741–4750.

Shepherd RK, Hardie NA (2001) Deafness-induced changes in the auditory pathway: implications for cochlear implants. Audiol Neurootol 6:305–318.

Shigemoto T, Ohmori H (1991) Muscarinic receptor hyperpolarizes cochlear hair cells of chick by activating Ca^{2+}-activated K^{+} channels. J Physiol (Lond) 420:127–148.

Simmons DD (2002) Development of the inner ear efferent system across vertebrate species. J Neurobiol 53:228–250.

Simmons DD, Morley BJ (1998) Differential expression of the alpha 9 nicotinic acetylcholine receptor subunit in neonatal and adult cochlear hair cells. Brain Res Mol Brain Res 56:287–292.

Skellett RA, Crist JR, Fallon M, Bobbin RP (1995) Caffeine-induced shortening of isolated outer hair cells: an osmotic mechanism of action. Hear Res 87:41–48.

Slepecky N, Ulfendahl M, Flock A (1988) Effects of caffeine and tetracaine on outer hair cell shortening suggest intracellular calcium involvement. Hear Res 32:11–21.

Sridhar TS, Brown MC, Sewell WF (1997) Unique postsynaptic signaling at the hair cell efferent synapse permits calcium to evoke changes on two time scales. J Neurosci 17:428–437.

Sun Y, Qi X, Witte DP, Ponce E, Kondoh K, Quinn B, Grabowski GA (2002) Prosaposin: threshold rescue and analysis of the "neuritogenic" region in transgenic mice. Mol Genet Metab 76:271–286.

Vetter DE, Liberman MC, Mann J, Barhanin J, Boulter J, Brown MC, Saffiote-Kolman J, Heinemann SF, Elgoyhen AB (1999) Role of α9 nicotinic ACh receptor subunits in the development and function of cochlear efferent innervation. Neuron 23:93–103.

Wiechers B, Gestwa G, Mack A, Carroll P, Zenner HP, Knipper M (1999) A changing pattern of brain-derived neurotrophic factor expression correlates with the rearrangement of fibers during cochlear development of rats and mice. J Neurosci 19:3033–3042.

Wiederhold ML, Kiang NY (1970) Effects of electric stimulation of the crossed olivocochlear bundle on single auditory-nerve fibers in the cat. J Acoust Soc Am 48:950–965.

Yamamoto T, Kakehata S, Yamada T, Saito T, Saito H, Akaike N (1995) Caffeine rapidly decreases potassium conductance of dissociated outer hair cells of guinea-pig cochlea. Brain Res 677:89–96.